

DOES THE SLIM-DISK MODEL CORRECTLY CONSIDER PHOTON-TRAPPING EFFECTS?

K. OHSUGA AND S. MINESHIGE

Yukawa Institute for Theoretical Physics, Kyoto University, Kyoto 606-8502, Japan

M. MORI

Institute of Natural Science, Senshu University, Kawasaki, Kanagawa 214-8580, Japan

AND

M. UMEMURA

Center for Computational Physics, University of Tsukuba, Tsukuba, Ibaraki 305-8577, Japan

Draft version October 28, 2018

ABSTRACT

We investigate the photon-trapping effects in the super-critical black hole accretion flows by solving radiation transfer as well as the energy equations of radiation and gas. It is found that the slim-disk model generally overestimates the luminosity of the disk at around the Eddington luminosity (L_E) and is not accurate in describing the effective temperature profile, since it neglects time delay between energy generation at deeper inside the disk and energy release at the surface. Especially, the photon-trapping effects are appreciable even below $L \sim L_E$, while they appear above $\sim 3L_E$ according to the slim disk. Through the photon-trapping effects, the luminosity is reduced and the effective temperature profile becomes flatter than $r^{-3/4}$ as in the standard disk. In the case that the viscous heating is effective only around the equatorial plane, the luminosity is kept around the Eddington luminosity even at very large mass accretion rate, $\dot{M} \gg L_E/c^2$. The effective temperature profile is almost flat, and the maximum temperature decreases in accordance with rise in the mass accretion rate. Thus, the most luminous radius shifts to the outer region when $\dot{M}/(L_E/c^2) \gg 10^2$. In the case that the energy is dissipated equally at any heights, the resultant luminosity is somewhat larger than in the former case, but the energy-conversion efficiency still decreases with increase of the mass accretion rate, as well. The most luminous radius stays around the inner edge of the disk in the latter case. Hence, the effective temperature profile is sensitive to the vertical distribution of energy production rates, so is the spectral shape. Future observations of high L/L_E objects will be able to test our model.

Subject headings: accretion: accretion disks — black hole physics — radiative transfer

1. INTRODUCTION

X-ray binary sources and active galactic nuclei (AGNs) emit enormous energy in radiation, and it is believed that the accretion disks are the main place of energy release in those objects. The standard-disk model was proposed by Shakura & Sunyaev (1973) as a very efficient conversion mechanism of gravitational energy of accreting gas into radiation energy (Pringle 1981; Frank, King, & Raine 1985; Kato, Fukue, & Mineshige 1998). The standard model has been very successful in describing optically thick flow structure, as long as the mass accretion rate, \dot{M} , is less than the critical mass accretion rate, $\dot{M}_{\text{crit}} \equiv L_E/c^2$, with L_E being the Eddington luminosity given by $4\pi cGMm_p/\sigma_T$, where c is the light velocity, M is the black hole mass, m_p is the proton mass, and σ_T is the Thomson scattering cross-section. However, sub-critical accretion is not always guaranteed, since the mass accretion rate is determined by something other than the central star itself, i.e., companion star in binary system (Alme & Wilson 1976; Spruit & Ritter 1983; King et al. 1997; Koyama et al. 1999) or circumnuclear star clusters in AGNs (Norman & Scoville 1988; Umemura, Fukue, & Mineshige 1998; Ohsuga et al. 1999). Therefore, it is no wonder that the mass accretion rate can greatly exceed the critical value.

When the mass accretion rate is comparable to or more

than the critical limit, the disk becomes radiation pressure dominant. In the case of $\dot{M} \gtrsim 10\dot{M}_{\text{crit}}$, moreover, the disk is moderately geometrically thick and advective energy transport becomes substantial. Such a disk is called a slim disk and has been investigated in detail (Abramowicz et al. 1988; Szuszkiewicz, Malkan, & Abramowicz 1996; Wang et al. 1999; Watarai & Fukue 1999; Watarai et al. 2000). The unique feature in high $\dot{M}/\dot{M}_{\text{crit}}$ systems is that photons are trapped (Katz 1977; Begelman 1978; Begelman & Meier 1982; Flammang 1984; Blondin 1986; Colpi 1988; Wang & Zhou 1999). In optically thick accretion flow, frequent interaction between matter and photons delays liberation of the radiation energy arising at deeper inside the disk. Thus, the radiation energy is trapped in the flow and advected inward. Such a photon-trapping plays an important role when the radiative diffusion time-scale is longer than the accretion time-scale. Since the trapped radiation energy can fall onto the black hole with the accreting gas without being radiated away, the observed luminosity is reduced in the black-hole accretion flow. In contrast, the advected energy should be finally radiated at the stellar surface in the case of neutron star (Houck & Chevalier 1992).

While most studies focused on spherical accretion case with some discussion on Comptonization, we here focus on the disk accretion case. In the slim-disk approach, the

vertically-integrated approximation is adopted; namely the radiative flux at the disk surface is related to the temperature on the equatorial plane, T_c , through the relation, $F_{\text{surf}}^z \sim \sigma T_c^4 / \tau$, where σ is the Stefan-Boltzmann constant and τ is the vertical Thomson scattering optical depth for a half of the disk. However, this holds only when the radiative diffusion time-scale is shorter than the accretion time-scale. In other words, the photon-trapping effects are not exactly taken into consideration in the slim-disk formulation. Eggum, Coroniti, & Katz (1987, 1988) initiated the two-dimensional radiation-hydrodynamical simulations by assuming the equilibrium between gas and radiation. Recently, the improved simulations, in which the energy of gas and radiation are separately treated, were performed by Okuda, Fujita, & Sakashita (1997), Fujita & Okuda (1998) and Kley & Lin (1999).

In this work, by solving radiation transfer, we investigate the photon-trapping effects, paying attention to energy transmission inside the disk in the optically-thick black hole accretion flows. The validity of the slim-disk model is also discussed in terms of the luminosity and the effective temperature profile. In §2, we present basic considerations of the photon-trapping effects based on the comparison of the accretion time-scale and the radiative diffusion time-scale. Model and basic equations for numerical simulations are given in §3, and we describe results in §4. Finally, §5 and §6 are devoted to discussion and conclusions.

2. BASIC CONSIDERATIONS

The radiation energy generated near the equatorial plane diffuses toward the disk surface at the speed of $\sim c/3\tau$ (Mihalas & Mihalas 1984), so that the time-scale of radiative diffusion is $t_{\text{diff}} = H/(c/3\tau)$, where H is the disk half-thickness. Since the accretion time-scale, t_{acc} , is given by $-r/v_r$, the condition that the radiation energy in the disk is trapped in the flow and falls onto the black hole is written as $H/(c/3\tau) \gtrsim -r/v_r$, where r is the radius and v_r is the accretion velocity of the flow. Using the relation, $\tau = \sigma_T \Sigma / 2m_p$, and the continuity equation of the accretion disk, $\dot{M} = -2\pi r v_r \Sigma$, we obtain the photon-trapping radius as

$$r_{\text{trap}} = \frac{3}{2} \dot{m} r_g h, \quad (1)$$

where Σ is the surface density of the disk, \dot{m} is the mass accretion rate normalized by the critical mass accretion rate, $\dot{m} \equiv \dot{M}/\dot{M}_{\text{crit}}$, r_g is the Schwarzschild radius, and h is the ratio of the half disk-thickness to the radius $h = H/r$, respectively. Hence, the photon-trapping effects perform significant role in the super-critical accretion flow when $r_{\text{trap}} > 3r_g$, namely at $\dot{m} \gtrsim 2$, since h is of the order of unity in radiation pressure dominant region.

The energy dissipated by viscosity at the regions of $r < r_{\text{trap}}$ can not be released but is carried onto the black hole, as long as the radiative diffusion is the predominant process for energy transport. Since the radiation arising merely at $r > r_{\text{trap}}$ can pass through the disk body to go out from the surface, the luminosity is roughly estimated by

$$L \sim 2 \int_{\max[r_{\text{in}}, r_{\text{trap}}]}^{\infty} 2\pi r Q_{\text{vis}} dr, \quad (2)$$

where r_{in} is the inner edge of the disk, Q_{vis} is the half vertically-integrated viscous heating rate, and the compressional heating is neglected. Adopting the viscous heating rate as

$$Q_{\text{vis}} \sim \frac{3}{8\pi} \Omega_K^2 \dot{M} \left[1 - \left(\frac{r_{\text{in}}}{r} \right)^{1/2} \right] \quad (3)$$

(Shakura & Sunyaev 1973; Lynden-Bell & Pringle 1974), with Ω_K being the Keplerian angular speed, we have in Newtonian approximation

$$L \sim \frac{r_g}{4r_{\text{in}}} \dot{M} c^2, \quad (4)$$

for $\dot{m} \ll 2r_{\text{in}}/(3r_g h)$, and

$$L \sim \frac{3}{4} \dot{M}_{\text{crit}} c^2 \left[\frac{2}{3h} - \frac{2}{3} \left(\frac{2}{3h} \right)^{3/2} \left(\frac{r_{\text{in}}}{r_g \dot{m}} \right)^{1/2} \right], \quad (5)$$

if \dot{m} is larger than $2r_{\text{in}}/(3r_g h)$. It is found in the limit of large \dot{m} ($\gg 1$) that the luminosity is roughly constant irrespective of \dot{m} so that the energy-conversion efficiency, $\eta \equiv L/\dot{M}c^2 \sim \dot{M}_{\text{crit}}/2\dot{M}h = (2h\dot{m})^{-1}$, should be remarkably reduced in the super-critical accretion disk with $\dot{m} \gg 1$. Also, it is important to note that the photon-trapping effects do not depend on the accretion velocity nor viscosity for a fixed \dot{m} , since the accretion velocity increases if α rises, but at the same time, the radiative diffusion velocity also increases in accordance with decrease in the surface density of the disk (i.e., $\Sigma \propto v_r^{-1} \propto \alpha^{-1}$).

So far, we have considered the limiting model that the viscous heating occurs only in the vicinity of the equatorial plane. Next, we investigate the photon-trapping effects for the model that the gas is heated up in proportion to the density. Just as in the previous model, the photon-trapping effects are appreciable within the trapping radius, however, the radiation arising near the disk surface is not trapped in the flow. The condition for the photon trapping to occur at z is given by $(H-z)/(c/3\tau_z) \gtrsim -r/v_r$, where z is the vertical height and τ_z is the vertical optical depth measured from the surface of the disk, $\tau_z \equiv \int_z^{\infty} (\rho \sigma_T / m_p) dz$, with ρ being the gas density. Assuming that the gas density is constant in the vertical direction for simplicity, namely $\tau_z = \tau(H-z)/H$, and using the continuity equation of the accretion disk as well as equation (1), we find that the energy dissipated at $\tau_z < (r/r_{\text{trap}})^{1/2} \tau$ can be radiated away even within the trapping radius. Therefore, the luminosity is estimated by

$$\begin{aligned} L &\sim 2 \int_{r_{\text{in}}}^{r_{\text{trap}}} 2\pi r Q_{\text{vis}} \left(\frac{r}{r_{\text{trap}}} \right)^{1/2} dr + 2 \int_{r_{\text{trap}}}^{\infty} 2\pi r Q_{\text{vis}} dr \\ &= \frac{3}{4} \dot{M}_{\text{crit}} c^2 \left[-\frac{2}{3h} + \frac{1}{3} \left(\frac{2}{3h} \right)^{3/2} \left(\frac{r_{\text{in}}}{\dot{m} r_g} \right)^{1/2} \right. \\ &\quad \left. + \left(\frac{2\dot{m} r_g}{3hr_{\text{in}}} \right)^{1/2} \right], \quad (6) \end{aligned}$$

when $\dot{m} > 2r_{\text{in}}/(3r_g h)$. In this model, the luminosity is not constant but depends on the mass accretion rate as $\propto \dot{m}^{1/2}$ at $\dot{m} \gg 1$. The energy-conversion efficiency decreases as $\eta \propto \dot{m}^{-1/2}$. If $\dot{m} < 2r_{\text{in}}/(3r_g h)$, the photon-trapping effects do not appear and the observed luminosity is given by equation (4). Here, it is stressed that the assessment with using the radiative diffusion velocity is

valid when the most of radiation energy arises at deeper inside the disk. If the viscous heating occurs only around the disk surface, the photon trapping would be ineffective. The reason of this is that the photons arising at near disk surface ($\tau_z \ll 1$) can easily escape from the flow since an average number of the scatterings is $\sim \tau_z$, in spite of τ_z^2 for photons emitted at $\tau_z \gg 1$ (Sunyaev & Titarchuk 1985).

In Figure 1, we show the expected luminosity changes as functions of \dot{m} assessed from equations (4), (5), and (6). To compare with the numerical results (§4.2), the former and latter models are represented as the analytical models A (thick solid curve) and B (dashed curve), respectively, and $h = 0.5$ as well as $r_{\text{in}} = 3r_g$ are assumed. In the sub-critical regime, the luminosities for both models vary along the thin solid line. We also display the luminosity of the slim disk (dotted curve). These two models are both extreme in the opposite sense, and actual situation will lie just in between. We thus expect that the luminosity increases moderately but rises slowly than $\dot{m}^{1/2}$. Hence, the slim disk is expected to overestimate the luminosity at $L \gtrsim L_E$, namely $\dot{m} \gtrsim$ a few. In §4.2, we discuss about behavior of the luminosity in more detail. To assess the radiative flux as a function of radius, we need to calculate the radius, at which the energy emerged at outer region is released. Note that finite disk size effect enhances photon trapping, and the disks would be even fainter (see §5.2).

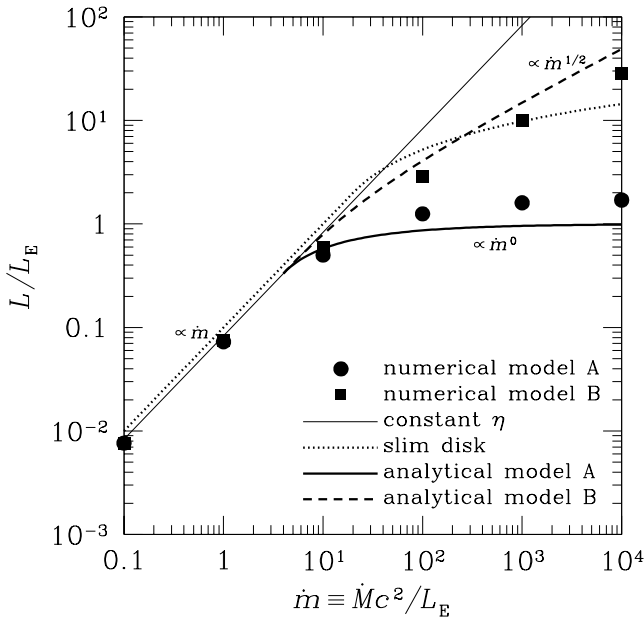


FIG. 1.— The luminosity is plotted against the mass accretion rate, where the luminosity and mass accretion rate are normalized by the Eddington luminosity and the critical mass accretion rate, respectively. The thick solid and dashed curves are the luminosities analytically estimated in §2. The circles and squares are the numerical results for models A and B, respectively. The luminosity should increase along the thin solid line, if energy-conversion efficiency is constant. It is found, however, that the energy-conversion efficient is on decrease in the super-critical accretion flow. Clearly, the slim disk (dotted curve) considerably overestimates the luminosity as compared with model A at whole super-critical regime and with model B when $\dot{m} \sim 10 - 10^3$. The numerical results are roughly consistent with analytical ones.

3. MODEL AND BASIC EQUATIONS FOR NUMERICAL SIMULATIONS

In the previous section, we roughly estimate the photon-trapping effects by comparing the accretion time-scale and the radiative diffusion time-scale. In this section, we examine the photon-trapping effects by practically solving radiation transfer, and the energy equations of gas and radiation. Since we are more concerned with the photon-trapping effects themselves rather than flow structure, we employ a simple model for the accretion flow. Here, the cylindrical coordinate, (r, φ, z) , is used. We consider that the accretion disk is axisymmetric and steady in the Eulerian description; $\partial/\partial\varphi = \partial/\partial t = 0$. The radial component of the velocity is expressed in terms of free-fall velocity as

$$v_r = -\xi \left(\frac{GM}{r} \right)^{1/2}, \quad (7)$$

where ξ is a constant parameter, and its vertical component is prescribed as

$$v_z = \frac{z}{r} v_r, \quad (8)$$

i.e., we assume convergence flow. Note that v_r is related to the viscosity parameter α through $v_r \sim \alpha (H/r) c_s$, where c_s is the sound velocity. We focus on the accreting ring element whose geometrical width and thickness are Δr and $2H$, respectively, where $\Delta r \ll r$ (see Figure 2). We suppose the structure of the accretion disk to be locally plane parallel, that is to say, each ring is composed of N layers in the z -direction, and the thickness of each layer is $\Delta z = 2H/N$. We solve the time-dependent energy fields of gas and radiation in the ring element during the course of accretion motion until the element reaches the inner edge of the disk. We adopt uniform density profile,

$$\rho(r, z) = \frac{\Sigma(r)}{2H(r)} = \text{const. in } z, \quad (9)$$

and consider both of the viscous heating and compressional heating due to converging inflow. Since the flow is steady ($\partial/\partial t = 0$), time coordinate can be transformed to the spatial coordinates; i.e., $D/Dt = v_r \partial/\partial r + v_z \partial/\partial z$ with v_r and v_z being given by equations (7) and (8). We thus express the radiative flux at the disk surface as a function of radius and then calculate the resultant luminosity of the disk.

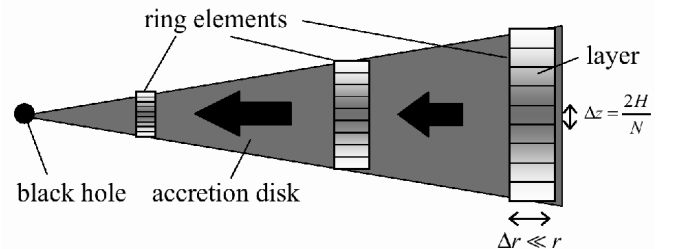


FIG. 2.— Schematic view of the black-hole accretion system explaining our calculation method. We calculate the evolution of the energy fields in a moving ring element that consists of N layers, until the element reaches the inner edge of the disk, assuming layers in each ring to be locally plane-parallel. Since the steady flow in the Eulerian description is considered, we set $\partial/\partial t = 0$, and thus replace $D/Dt = v_r \partial/\partial r + v_z \partial/\partial z$.

In plane parallel approximation, the radial and azimuthal components of the radiative flux are null. Also, non-diagonal components of the radiation stress tensor are null. Hence, using equations (7) and (8), we write the energy equations of radiation and gas as

$$\rho \left(v_r \frac{\partial}{\partial r} + \frac{z}{r} v_r \frac{\partial}{\partial z} \right) \left(\frac{E}{\rho} \right)$$

$$= -\frac{\partial F^z}{\partial z} + \frac{v_r}{r} \left(\frac{1}{2} P^{rr} - P^{\varphi\varphi} - P^{zz} \right) + 4\pi\kappa B - c\kappa E, \quad (10)$$

and

$$\rho \left(v_r \frac{\partial}{\partial r} + \frac{z}{r} v_r \frac{\partial}{\partial z} \right) \left(\frac{e}{\rho} \right) = -\frac{3}{2} \frac{v_r}{r} p_{\text{gas}} - 4\pi\kappa B + c\kappa E + q_{\text{vis}}, \quad (11)$$

respectively, where E is the radiation energy density, F^z is the radiative flux in the z -direction, P^{ii} is the diagonal components of the radiation stress tensor, κ is the absorption coefficient, B is the blackbody intensity written as $B = \sigma T_{\text{gas}}^4/\pi$ with T_{gas} being the gas temperature, e is the internal energy density, p_{gas} is the gas pressure, and q_{vis} is the viscous heating rate per unit volume (Mihalas & Klein 1982; Mihalas & Mihalas 1984; Fukue, Kato, & Matsumoto 1985; Stone, Mihalas, & Norman 1992). To close the set of equations, we apply the flux-limited diffusion approximation for the radiative flux and stress tensor,

$$F^z = -\frac{c\lambda}{\chi} \frac{\partial E}{\partial z}, \quad (12)$$

$$P^{rr} = P^{\varphi\varphi} = \frac{1}{2}(1-f)E, \quad (13)$$

and

$$P^{zz} = fE, \quad (14)$$

with χ being the extinction coefficient, where λ , R , and f are defined as

$$\lambda = \frac{2+R}{6+3R+R^2}, \quad (15)$$

$$R = \frac{1}{\chi E} \left| \frac{\partial E}{\partial z} \right|, \quad (16)$$

and

$$f = \lambda + \lambda^2 R^2 \quad (17)$$

(Turner & Stone 2001). This approximation holds both in the optically thick and thin regimes. In the optically thick limit, we find $\lambda \rightarrow 1/3$ and $f \rightarrow 1/3$ because of $R \rightarrow 0$. In the optically thin limit of $R \rightarrow \infty$, on the other hand, we have $|F^z| = cE$, $P^{rr} = P^{\varphi\varphi} = 0$, and $P^{zz} = E$. These give correct relations in the optically thick diffusion limit and optically thin streaming limit, respectively. Thus, we can rewrite the radiation energy equation (10) as

$$\rho \left(v_r \frac{\partial}{\partial r} + \frac{z}{r} v_r \frac{\partial}{\partial z} \right) \left(\frac{E}{\rho} \right) = c \frac{\partial}{\partial z} \left(\frac{\lambda}{\chi} \frac{\partial E}{\partial z} \right) - \frac{3f+1}{4} \frac{v_r}{r} E + 4\pi\kappa B - c\kappa E. \quad (18)$$

These nonlinear equations (11) and (18) are integrated iteratively by the Newton-Raphson method with the Gauss-Jordan elimination for a matrix inversion, by coupling with the continuity equation,

$$\dot{M} = -2\pi r v_r \Sigma, \quad (19)$$

the density profile given by equation (9), and the equation of state,

$$p_{\text{gas}} = \frac{2}{3}e. \quad (20)$$

As to the vertical distribution of viscous heating rates, we consider two extreme models. In model A, we assume that

the viscous heating is effective only in the vicinity of the equatorial plane at $|z| < 10^{-2}H$, that is to say,

$$q_{\text{vis}}(z) = \begin{cases} 10^2 Q_{\text{vis}}/H & |z| \leq 10^{-2}H \\ 0 & |z| > 10^{-2}H \end{cases}, \quad (21)$$

where Q_{vis} is given by equation (3). In model B, we assume that the gas is heated up uniformly, independently of z , that is,

$$q_{\text{vis}}(z) = \frac{Q_{\text{vis}}}{H} = \text{const.} \quad (22)$$

Throughout the present study, the black hole mass is fixed to be $10M_{\odot}$ and the inner edge of the disk is taken to be at $r_{\text{in}} = 3r_g$. Moreover, we assume H to be $0.5r$ (i.e., $h = 0.5$), and $N = 100$ is employed. This assumption of $H = 0.5r$ would be reasonable in the super-critical accretion regime, since H/r of the radiation pressure dominant disk becomes of the order of unity. In the sub-critical regime, on the other hand, H would be much smaller than r , but then the most of emergent energy can be released immediately without being trapped. Thus, our numerical simulations are valid in both super-critical and sub-critical accretion regimes for evaluating the radiative flux at the disk surface.

4. RESULTS

4.1. Reduction of the radiative flux

The radiative flux is reduced due to the photon trapping in the vicinity of the inner edge of the disk when $\dot{m} \gg 1$. Figure 3 shows the ratios of the radiative flux at the disk surface, F_{surf}^z , to the vertically-integrated viscous heating rate for several \dot{m} as functions of radius. The solid and dashed curves correspond to model A and model B, respectively. Here, we consider the situation that the Thomson scattering is predominant over the absorption, $\kappa = 10^{-2}\rho\sigma_{\text{T}}/m_p$. We set ξ in equation (7) for different \dot{m} to be $(\dot{m}, \xi) = (0.1, 10^{-4})$, $(1, 10^{-3})$, $(10, 10^{-3})$, $(10^2, 10^{-2})$, $(10^3, 10^{-2})$, and $(10^4, 0.1)$ in order for the disk to be optically thick for Thomson scattering. Then, the viscosity parameter α is of the order of 10^{-4} in $\xi = 10^{-4}$ and 0.1 in $\xi = 0.1$, since $\alpha \sim \xi/h^2$ from equations (7) and (8). As shown in Figure 3, the ratio of $F_{\text{surf}}^z/Q_{\text{vis}}$ is around unity when the accretion rate is sub-critical, $\dot{m} \lesssim 1$. In the super-critical accretion disk, $\dot{m} \gg 1$, on the other hand, the ratio is much smaller than unity in the vicinity of the inner edge of the disk, but is still close to unity at the outer region. The ratio rises at $r \sim 3r_g$ again, but this rise is caused by the decline of Q_{vis} near the inner boundary. The absolute value of the radiative flux is still suppressed there.

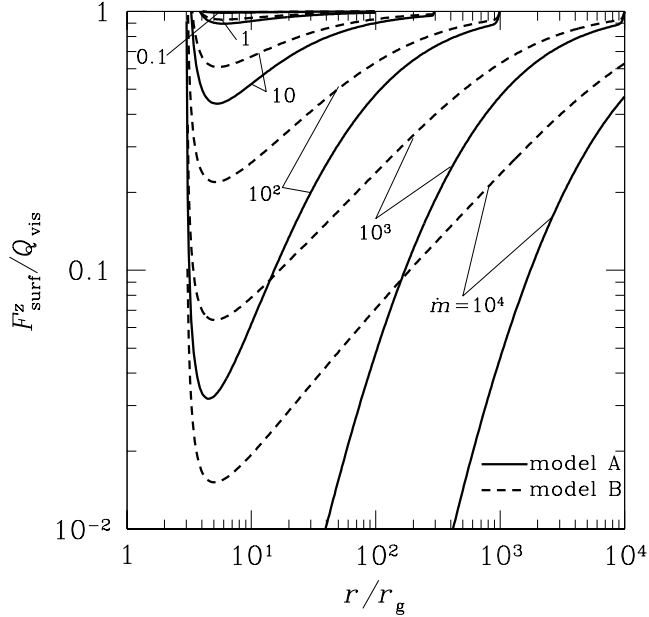


FIG. 3.— The ratios of radiative flux at the disk surface to the vertically integrated viscous heating rate as functions of radius for $\dot{m} = 0.1, 10, 10^2, 10^3$, and 10^4 . Here, the radius is normalized by the Schwarzschild radius. The solid and dashed curves indicate models A and B, respectively. By the photon-trapping effects, the ratios are much smaller than unity at the regions of $r < r_{\text{trap}}$ in the case of $\dot{m} \gg 1$, where r_{trap} is the photon-trapping radius given by equation (1). It is also found that the photon-trapping effects are more conspicuous in model A than in model B. If $\dot{m} \leq 1$, on the other hand, we found $F_{\text{surf}}^z / Q_{\text{vis}} \sim 1$, as in the standard disk.

This reduction of the radiative flux is due to the photon trapping, and it can be understood by the time delay owing to energy transport in the optically thick medium. The emergent radiation energy is diffused at the speed of $\sim c/3\tau$, and arrives at the disk surface after t_{diff} . If this time delay is comparable to or longer than the accretion time-scale, $t_{\text{diff}} \gtrsim t_{\text{acc}}$, the generated radiation energy is advected inward, so that the ratio of $F_{\text{surf}}^z / Q_{\text{vis}}$ should deviate from unity. To conclude, the energy dissipated by viscosity can be released from the surface immediately at the same radius, as in the standard disk, only in the outer region for $\dot{m} \gtrsim 1$ but in the whole region for $\dot{m} < 1$, where the radiative diffusion time-scale is much shorter than the accretion time-scale.

As shown in Figure 3, the photon-trapping effects are appreciable within $\dot{m}r_g$ in both models A and B. This is good agreement with the analytical prediction of r_{trap} , [see equation (1)]. However, the photon-trapping effects are more conspicuous in model A than in model B, since in model B the energy dissipated near the disk surface can still escape from the accretion flow even within the trapping radius. In model A, in contrast, most of energy is dissipated in the vicinity of the equatorial plane and is trapped in the flow. Realistic situation will be just in between.

Here, it should be stressed again that the photon-trapping effects themselves depend on \dot{m} and are independent of v_r , when \dot{m} is fixed, as was mentioned in §2, unless the disk is optically thin. To check if this is the case, we examine the cases with different ξ values; $\xi = 10^{-3}$ and 0.1, besides $\xi = 10^{-2}$, for $\dot{m} = 10^2$, finding no changes.

[However, if the absorption coefficient is very small, the luminosity would decrease in the case of rapid accretion, since thermal energy of the gas can not be converted into radiation energy (see §4.6).]

4.2. Luminosity

The luminosity of the disk is significantly reduced by the photon-trapping effects. In Figure 1, the calculated luminosity is also plotted against \dot{m} with symbols. Here, the circles and squares indicate the luminosities for models A and B, respectively. The thin solid line represents the luminosity expected on the assumption of the constant energy-conversion efficiency (η). In model A, the luminosity is kept around the Eddington luminosity irrespective of the mass accretion rate in the super-critical accretion regime, although the luminosity is in proportion to the mass accretion rate in the sub-critical accretion disk. Thus, the energy-conversion efficiency is remarkably reduced in the super-critical accretion due to significant photon-trapping effects, $\eta \sim \dot{m}^{-1}$. The calculated luminosity in model B in the super-critical regime is larger than in model A owing to relatively ineffective photon trapping. Even so, the energy-conversion efficiency is also categorically on decrease in the super-critical accretion regime, $\eta \propto \dot{m}^{-1/2}$. In both models, the results are in good agreement with the analytical estimates (§2).

The dotted curve is the luminosity calculated based on the slim-disk model (Watarai, Mizuno, & Mineshige 2001). The energy is assumed to be mainly dissipated on the equatorial plane in the slim disks, however, the luminosity of the slim disk is not kept around the Eddington luminosity but increases with the mass accretion rate. Hence, the slim disks considerably overestimate the luminosity compared with our similar model (model A). The luminosity is also larger in the slim disk than in model B in the region of $\dot{m} = 10 - 10^3$. The photon-trapping effects are already appreciable at $L \lesssim L_E$, while they are only substantial at $L \gtrsim L_E$ in the slim-disk treatment. The slim-disk model thus underestimates the photon trapping (see §1).

Numerical results are roughly consistent with the analytical assessments plotted based on equations (5) and (6), but deviations originate for the following reason. In numerical simulations, the energy transport at each height is actually solved by taking radiation transfer into consideration. On the other hand, the analytical assessments are merely obtained by the comparison of the accretion time-scale and the radiative diffusion time-scale.

4.3. Effective temperature

Since photon trapping tends to lower F_{surf}^z at smaller radii, the disk with super-critical accretion rate has a flatter effective temperature profile in the vicinity of the inner edge. We calculate the effective temperature, $T_{\text{eff}} \equiv [F_{\text{surf}}^z / \sigma]^{1/4}$, and plot in Figure 4 the effective temperature distributions for model A (solid curves) and model B (dashed curves), respectively. Although we adopt $M = 10M_\odot$, the results can be applied to cases with other M , if we vary the absolute value of T_{eff} in proportion to $M^{-1/4}$. The effective temperature for low \dot{m} , $\dot{m} = 0.1$ and 1, is proportion to $r^{-3/4}$ as in the standard disk (Shakura & Sunyaev 1973; Pringle 1981), since the photon-trapping effects are not appreciable when the mass accretion rate

is sub-critical (see Figure 3). In the case of the super-critical accretion disk, the slope of the effective temperature profile becomes flatter within the trapping radius, though we still have $T_{\text{eff}} \propto r^{-3/4}$ at $r > r_{\text{trap}}$. For $\dot{m} > 10^3$ in model A, especially, the profile within the trapping radius is almost flat and the maximum temperature begins to decrease with farther rise in \dot{m} . This makes a marked difference from the prediction by the slim disk, which shows $T_{\text{eff}} \propto r^{-1/2}$ in the high \dot{m} limit (Watarai & Fukue 1999; Watarai et al. 2000; discussed later)

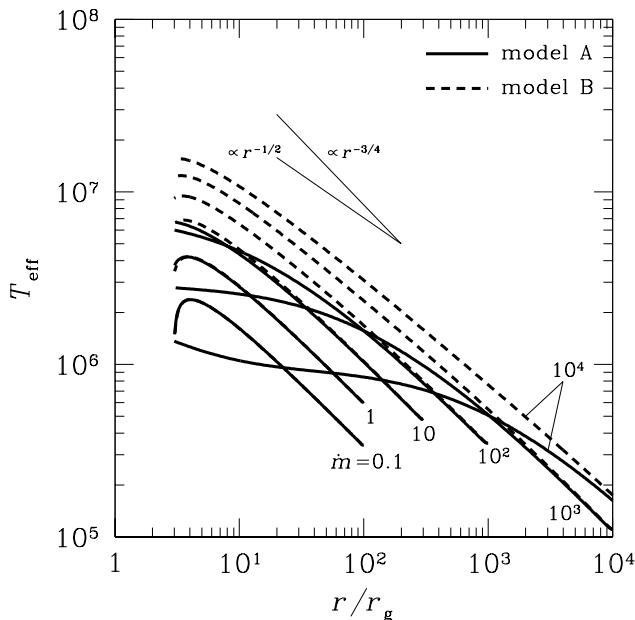


FIG. 4.— The effective temperature profile for model A (solid curves) and for model B (dashed curves) for various values of \dot{m} . In the case of $\dot{m} \leq 1$, the effective temperature is proportion to $r^{-3/4}$, as in the standard disk. However, the profile drastically changes in the super-critical accretion flow ($\dot{m} \gg 1$), and becomes significantly flatter at the region of $r < r_{\text{trap}}$. In model A, the maximum temperature decreases with increase in the mass accretion rate and the profile is nearly flat when $\dot{m} > 10^3$.

4.4. Spectral index

As we have seen above, the effective temperature profile is very sensitive to the functional form of $q_{\text{vis}}(z)$. The vertical distribution of viscous heating rates would be observationally distinguished when the luminosity is comparable to or more than the Eddington luminosity. The spectral energy distribution (SED) is strongly affected by the effective temperature profile, which in turn depends on $q_{\text{vis}}(z)$. We have calculated expected SED based on a superposition of blackbody spectra, $B_\nu[T_{\text{eff}}(r)]$, emitted from the disk surface, and plot in Figure 5 the spectral index, $\zeta = d \log L_\nu / d \log \nu$, in the range between 0.1 keV and 1.0 keV, as a function of the luminosity normalized by the Eddington luminosity. Here, the circles and squares indicate the spectral indices for models A and B, respectively. It is known that the spectrum of the standard type disk but with $T_{\text{eff}} \propto r^{-p}$ is composed of three components: Rayleigh-Jeans part ($L_\nu \propto \nu^2$) at low ν , Wien part [$\propto \nu^3 \exp(-h\nu/kT_{\text{eff}})$] at high ν , and a power-law part ($\propto \nu^{3-2/p}$) in the intermediate frequencies (Kato, Fukue, & Mineshige 1998), where ν is the photon frequency, h is the Planck constant, and k is the Boltzmann constant.

Thus, difference in p should manifest in this middle part.

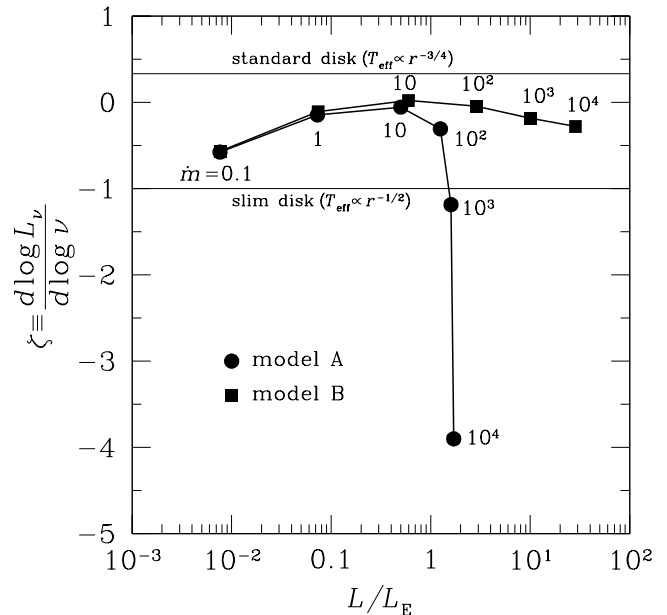


FIG. 5.— The spectral indices as functions of normalized luminosity, L/L_E . Here, we define the spectral index as $\zeta = d \log L_\nu / d \log \nu$ at 0.1–1.0 keV. The circles and squares correspond to models A and B, respectively. The spectral index is sensitive to the distributions of the viscous heating rates in the vertical direction, thus it can be determined observationally.

The effective temperature for $\dot{m} = 0.1$ and 1 is proportional to $r^{-3/4}$, however, the index deviates from $\zeta = 1/3$ for $p = -3/4$ expected from the standard-disk model, since we see a Wien cut-off on the high-frequency side. The effective temperature profile in model A becomes flatter and the maximum temperature begins to decrease when $\dot{m} > 10^2$, so that the peak of the SED shifts to the low-frequency side. Thus, the index drastically decreases in accordance with increasing \dot{m} , although the luminosity stays around the Eddington luminosity. In model B, on the other hand, the maximum temperature continues to increase with rise in the mass accretion rate. Therefore, the Wien cut-off is out of the range in the super-critical accretion. As shown in Figure 4, the effective temperature profile in model B is flatter than in the standard disk, $\propto r^{-3/4}$, but steeper than in the slim disk of high \dot{m} limit, $\propto r^{-1/2}$. Therefore, the index is settled down between $1/3$ (standard disk) and -1 (slim disk), and the luminosity increases in accordance with rise in the mass accretion rate. We can thus obtain information of $q_{\text{vis}}(z)$ by the X-ray observations of luminous X-ray objects.

4.5. Most luminous radius

The radius, at which differential luminosity [$(dL/dr)\Delta r$] is maximum, is at $(75/16)r_g$ in the standard disk. This 'most luminous radius' does not necessarily coincide with the inner edge radius, if the photon trapping is effective, since it is more prominent at small radii. We show the most luminous radii, r_{max} , normalized by r_g in Figure 6. The circles and squares indicate r_{max}/r_g for model A and model B, respectively. This figure clearly demonstrates for model A that the larger \dot{m} is, the larger becomes the most luminous radius, as long as $\dot{m} \gg 10^2$. In model B, the most luminous radius stays at around the inner

edge of the disk, but the photon trapping significantly reduces the overall radiative flux within the trapping radius.

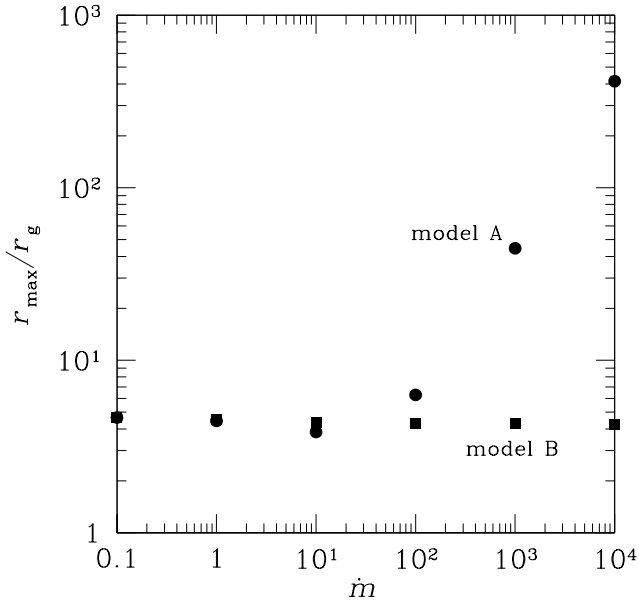


FIG. 6.— The most luminous radii, at which $(dL/dr)\Delta r$ is maximum, normalized by r_g are shown as functions of normalized mass accretion rate, \dot{m} . The circles and squares correspond to models A and B, respectively. Since the photon-trapping effects are most appreciable in the vicinity of the inner edge, the most luminous radius shifts from the inner edge to the outer region at high \dot{m} in model A. In model B, in contrast, the innermost ring is still most luminous, although the radiative flux at the surface is reduced within r_{trap} (see Figure 3).

4.6. Rapid accretion

So far, since we adopt relatively large absorption coefficient, the gas is approximately in equilibrium with radiation, $T_{\text{gas}} \sim T_{\text{rad}}$, where T_{rad} is the radiation temperature. Thus, the energy dissipated by viscosity can be promptly converted into radiation energy, and that energy is transported toward the disk surface by radiation transfer. However, if the absorption coefficient is much smaller, as in the case that we adopt free-free absorption, it is possible that the energy dissipated by viscosity is kept as thermal energy and is not converted into radiation energy. Therefore, the resultant luminosity must further decrease because of this effect in addition to the photon-trapping effects, if the gas accretes onto the black hole without achieving radiative equilibrium. This occurs, when α is relatively large $\alpha \gtrsim 0.03$ (Beloborodov 1998).

To demonstrate this phenomenon, we employ the Rosseland mean of the free-free absorption coefficient, $\kappa_{\text{ff}} = 1.7 \times 10^{-25} T_{\text{gas}}^{-7/2} (\rho/m_p)^2$ (Rybicki & Lightman 1979), and calculate and plot the luminosity against the radial velocity for model A (circles) and model B (squares) in Figure 7, where the mass accretion rate is fixed to be $\dot{m} = 10^2$. It is found that the accretion disk gets much fainter at the regime of $\xi = v_r/v_{\text{ff}} > 10^{-2}$ [corresponding to $\alpha \gtrsim 0.04$ if $H/r \sim 0.5$, since $v_r \sim \alpha(H/r)^2 v_{\text{ff}}$], where v_{ff} is the free-fall velocity. The accretion disks with huge accretion rate and large radial velocity tend to have extremely small energy-conversion efficiency and would be identified as faint objects. Note, however, that this criterion

of the radial velocity might vary, depending on the vertical density profile, since the free-free absorption coefficient strongly depends on the gas density, as well as the gas temperature. If the density and temperature of the gas is high around the equatorial plane, the thermal energy would be converted into the radiation energy there, and the disk might be somewhat brighter. Anyhow, the disk tends to be fainter in more rapid accretion in cooperation with the photon-trapping effects, although the detail examination requires multi-dimensional radiation-hydrodynamical simulation. (This will be performed in future.)

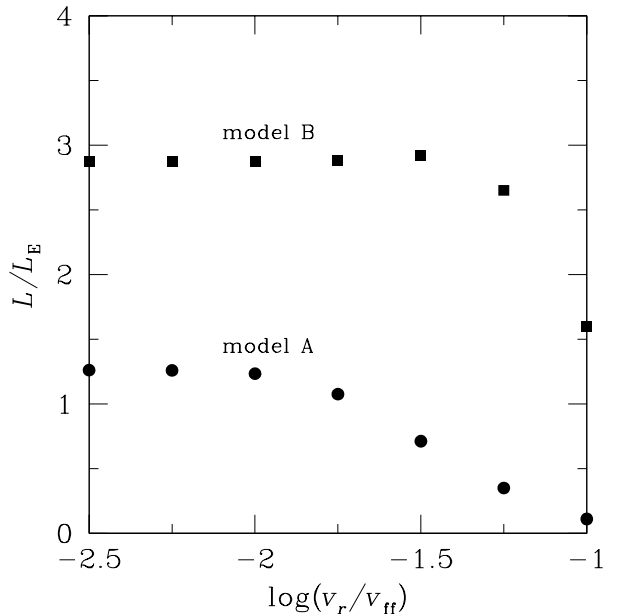


FIG. 7.— The luminosity of the flow as a function of the accretion velocity, where the circles and squares indicate model A and model B, respectively. Here, we adopt the Rosseland mean of the free-free absorption coefficient. The accretion disk becomes dimmer in the regime of $v_r > 10^{-2} v_{\text{ff}}$ ($\xi > 10^{-2}$), since the energy dissipated by viscosity is not sufficiently converted into radiation energy but kept as thermal energy of the gas. The luminosity of the accretion disk is suppressed by this effect as well as the photon-trapping effects in the case of the disk with rapid accretion (i.e., large $\alpha \gtrsim 0.04$).

5. DISCUSSION

5.1. Comparison with the slim-disk model

As a model for describing super-critical disk accretion flow, slim disks are often utilized. However, we wish to note that the slim disk does not accurately treat the photon-trapping effects in the disk accretion case. The slim disk can describe the dynamical structure of the flow reasonably well, since the energy balance is given by $Q_{\text{vis}} \sim Q_{\text{adv}}$ and does not depend on the radiative loss. The slim disk is not able to correctly estimate the radiative flux at the disk surface, in the sense that it overestimates the luminosity in all ranges in comparison with model A, and in the range of \dot{m} between 10 and 10^3 in model B. Moreover, we found that the effective temperature profile becomes significantly flatter in model A, but slightly steeper in model B, $T_{\text{eff}} \propto r^{-p}$ with $p > 1/2$. Hence, the profile strongly depends on the distribution of viscous heating rates.

The deviations of our results from the slim disk originate for the following reason. In the slim disk, using

the vertically-integrated approximation, the accreting velocity of the flow is investigated by solving the equation of motion in the r -direction, and the radiative flux from the disk surface is determined as a function of radius so as to satisfy the vertically integrated energy equation, $Q_{\text{vis}} = \sigma T_{\text{eff}}^4 + Q_{\text{adv}}$, where Q_{adv} is the advective cooling term. The resultant luminosity increases in accordance with rise in the mass accretion rate, and the effective temperature profile is obtained as $T_{\text{eff}} \propto r^{-1/2}$ in the limit of large \dot{m} . However, the radiative flux from the disk surface is assumed to be related to the temperature on the equatorial plane as $\sigma T_{\text{eff}}^4 \sim \sigma T_c^4 / \tau$. Since the radiation energy produced near the equatorial plane can not be radiated away immediately at the same radius but is advected inward at $r < r_{\text{trap}}$, the effective temperature in reality does not always reflect the temperature of the equatorial plane at the same radius. The relation of $\sigma T_{\text{eff}}^4 \sim \sigma T_c^4 / \tau$ actually holds, only when the photon-trapping is not appreciable. Hence, the slim disk cannot give the accurate radiative flux at the disk surface, although a part of the photon-trapping effects, the advection of the energy, is taken into consideration in the equation of energy balance. In the present study, on the other hand, we have actually solved radiative transfer in the z -direction (in the comoving frame) to investigate the radiative flux from the disk surface. Consequently, the observed luminosity and the effective temperature profile deviate from the prediction of the slim disk.

5.2. Future work

We have so far assume that the disk size is practically infinite, but the super-critical accretion disk would be much dimmer when the disk size, r_{out} , is smaller than the trapping radius. In model A, most of energy arises near equatorial plane of the disk, and thus cannot arrive at the disk surface if $r_{\text{trap}} > r_{\text{out}}$. As a result, the luminosity in such a case must be extremely small, $L \ll L_E$. In model B, the luminosity is estimated as

$$\begin{aligned}
 L &\sim 2 \int_{r_{\text{in}}}^{r_{\text{out}}} 2\pi r Q_{\text{vis}} \left(\frac{r}{r_{\text{trap}}} \right)^{1/2} dr \\
 &= \frac{3}{4} \dot{M}_{\text{crit}} c^2 \left(\frac{2\dot{m}}{3h} \right)^{1/2} \\
 &\quad \times \left[-2 \left(\frac{r_g}{r_{\text{out}}} \right)^{1/2} + \left(\frac{r_g}{r_{\text{in}}} \right)^{1/2} + \left(\frac{r_{\text{in}} r_g}{r_{\text{out}}^2} \right)^{1/2} \right] \quad (23)
 \end{aligned}$$

when $r_{\text{trap}} > r_{\text{out}}$. For example, this equation indicates $L/L_E \sim 3.1$ and 0.11 for $r_{\text{out}} = 10^2 r_g$ and $10 r_g$, respectively, in comparison with $L/L_E \sim 30$ for the case of $r_{\text{out}} \gg r_{\text{trap}}$, where we assume $r_{\text{in}} = 3r_g$, $\dot{m} = 10^4$, and $h = 0.5$. Such a situation might be realized in the accretion disks in the compact binaries, in the central regions of Type II supernovae (e.g., Mineshige et al. 1997) and in gamma-ray bursts (e.g., Narayan, Piran, & Kumar 2001).

Throughout the present study, we describe the simple model for accretion motion without treating the hydrodynamical simulations. If the radiative flux force at the disk surface is stronger than the gravity of the black hole, the gas will be blown out like a wind (Eggum, Coroniti, & Katz 1987, 1988; Okuda, Fujita, & Sakashita 1997; Fujita & Okuda 1998). Since the ratio of the radiative flux force

to the gravity in the z -direction is roughly estimated as $\sim \dot{m}(r/r_g)^{-1} F_{\text{surf}}^z / Q_{\text{vis}}$, the photon-trapping effects tend to prevent outflow by suppression of $F_{\text{surf}}^z / Q_{\text{vis}}$. Indeed, the gas would accrete onto the black hole without being blown out in model A (see Figure 3). Further study demands multi-dimensional radiation-hydrodynamical simulation.

Moreover, we notice two very important improvement to be made. One is to include convection effect, which seems to occur when disk is radiation pressure-dominated (Shakura, Sunyaev, & Zilitinkevich 1978; Agol et al. 2001). Even if the viscous heating is effective in the vicinity of the equatorial plane as in model A, the convection might more efficiently transfer the energy from the equatorial plane to the disk surface than radiation. Then, resultant properties of the disk would become close to model B, but it is necessary for investigating in detail to solve two dimensional hydrodynamical equations coupled with radiation transfer. Second is to take the relativistic effect into consideration. It would play a significant role around the inner edge of the disk.

5.3. Observational implications

There seem to be several possible sites of super-critical accretion flow, where the photon-trapping effects may play a significant role. Firstly, we mention micro-quasars which compose a peculiar subclass of X-ray transients seemingly containing black holes (see Tanaka & Shibazaki 1996 for a review). There is an indication that they emit rather high luminosity, near Eddington. In the case of GRS 1915+105, for example, its black hole mass determination was done as $18.6 \pm 2.2 M_\odot$ by Borozdin et al. (1999) based on the model fitting of the X-ray spectra. Independently, Greiner, Cuby, & McCaughrean (2001) obtained $14 \pm 4 M_\odot$ through observations of Doppler shifted CO lines of the secondary star. Thus, its X-ray luminosity of several times 10^{39} erg s^{-1} at the peak is close to the Eddington luminosity of $(2.3 \pm 0.3) \times 10^{39}$ erg s^{-1} . Bursting behavior could be explained by relaxation oscillation between the slim and standard disk (Honma, Kato, & Matsumoto 1991; Yamaoka, Ueda, & Inoue 2001). If this is the case, this provides strong evidence for the presence of a super-critical accretion flow.

Second one is ultra luminous X-ray sources (ULXs). ULXs with intermediate-massive black holes are successively discovered in nearby galaxies and some of them seem to emit large luminosity, corresponding to the Eddington luminosity (Okada et al. 1998; Colbert & Mushotzky 1999; Mizuno et al. 1999; Makishima et al. 2000). In addition, an intermediate massive black hole of $\gtrsim 10^3 M_\odot$ which is discovered in M82 (Matsumoto et al. 2001) is also a good candidate of super-critical accretion, although it is not always clear if their luminosities are really close to the Eddington luminosities, since there is no accurate mass estimations.

Narrow-line Seyfert 1 galaxies (NLS1s), which are believed to have a central black hole, are also considered to be sites of super-critical accretion (Mineshige et al. 2000). Since the NLS1s exhibit large soft X-ray excess (Boller, Brandt, & Fink 1996; Otani, Kii, & Miya 1996; Leighly 1999; Hayashida 2000), mass of the central black hole is estimated as $M \sim 10^{5-7} M_\odot$ by a comparison with soft X-

ray bump in galactic black hole candidates. Such moderate mass is also supported by reverberation mapping (Laor et al. 1997) and X-ray variability method (Hayashida 2000), and is consistent with narrow Balmer lines of NLS1s. Thus, the observed luminosity, $L \sim 10^{43-44}$, is near the Eddington luminosity, and it implies that the accretion flow is super-critical.

The final candidate is gamma-ray bursts (GRBs) (Piran 1999, Mészáros, Rees, & Wijers 1999; Mészáros 2001). Interestingly, many models (such as mergers of double neutron stars, neutron star–black hole mergers, collapsars, and so on) predict a similar configuration as a final product; namely, a stellar-mass black hole surrounded by a massive torus with a mass of 0.01 – a few M_{\odot} . Then, gas accretion onto a new-born black hole may be the origin of huge energy release and high Lorentz factor (e.g. Narayan, Paczyński, & Piran 1992; Narayan, Piran, & Kumar 2001). A simple estimation gives an enormous mass accretion rate. If gas with mass of M_{gas} falls onto a black hole with a mass M on a time-scale of t_{acc} sec, we find $\dot{M} \simeq 2 \times 10^{33} (M_{\text{gas}}/M_{\odot}) (t_{\text{acc}}/1\text{s})^{-1} \text{g s}^{-1}$, that is,

$$\dot{m} = \dot{M} c^2 / L_E \sim 4 \times 10^{15} \left(\frac{M_{\text{gas}}}{M_{\odot}} \right) \left(\frac{M}{3M_{\odot}} \right)^{-1} \left(\frac{t_{\text{acc}}}{1\text{s}} \right)^{-1}, \quad (24)$$

(see, e.g., Narayan, Piran, & Kumar 2001). Then, the photon-trapping radius should be huge, $r_{\text{trap}} \sim 10^{15} r_g$. Since the disk size is, at most, about the size of giant stars, $r_{\text{out}} \sim 10^{13-14} \text{cm} \sim 10^{7-8} (M/3M_{\odot})^{-1} r_g$, it is very likely that the emission from the entire disk surface is totally blocked as we already mentioned, although neutrino energy loss may be essential in such a massive disk (Ruffert & Janka 1999; Popham, Woosley, & Fryer 1999).

6. CONCLUSIONS

By employing a simple accretion flow model, we have investigated the photon-trapping effects in the super-critical black hole accretion flows by solving radiation transfer and energy equations of gas as well as radiation. The present results are summarized as follows.

(1) The radiative flux at the disk surface is reduced within $\sim \dot{m} r_g$ due to photon trapping. Then, the luminosity is kept around the Eddington luminosity if the viscous heating is effective only in the vicinity of the equatorial

plane. Thus, the energy-conversion efficiency is drastically on decrease, $\eta \equiv L/Mc^2 \sim \dot{m}^{-1}$. Even if the energy is dissipated equally in the disk, the energy-conversion efficiency is also suppressed in accordance with rise in the mass accretion rate, $\eta \propto \dot{m}^{-1/2}$.

(2) The slim disk can not accurately describe the effective temperature profile, since it is assumed to be related to the temperature on the equatorial plane as $T_{\text{eff}} \sim T_c/\tau^{1/4}$. As a result, the slim disk overestimates the luminosity of the disk at $L \sim L_E$. The photon-trapping effects are already appreciable at the luminosities as low as $\lesssim L_E$, while they only become critical at $L \gtrsim 3L_E$ according to the slim disk calculations.

(3) Through the photon-trapping effects, the effective temperature profile becomes flatter than $T_{\text{eff}} \propto r^{-3/4}$ within the photon trapping radius in the super-critical accretion. If the energy is dissipated in the vicinity of the equatorial plane, the profile is almost flat ($T_{\text{eff}} \propto r^{-p}$ with $p \sim 0$) and the maximum temperature decreases in accordance with the rise in the mass accretion rate.

(4) The information regarding the distribution of the viscous heating rates, $q_{\text{vis}}(z)$, can be obtained through the observations of luminous X-ray objects at $L \gtrsim L_E$. In accordance with rise in the mass accretion rate, the spectral index, $\zeta = d \log L_{\nu} / d \log \nu$ [0.1 keV – 1.0 keV] for $M = 10M_{\odot}$, increases but in the different ways, depending the functional form of $q_{\text{vis}}(z)$. When the gas is heated up uniformly, independently of the vertical height, especially, the spectral index stays between -0.5 and 0 , although the index must be further small, $\ll -1$, in the case that the energy is dissipated around the equatorial plane. Moreover, the most luminous radius shifts to the outer region as long as $\dot{m} \gg 10^2$ in the latter case.

We are grateful to J. Fukue, T. Nakamoto, and K. Watarai, for helpful discussion. The calculations were carried out at Yukawa Institute for Theoretical Physics in Kyoto University. This work is supported in part by Research Fellowships of the Japan Society for the Promotion of Science for Young Scientists, 02796 (KO) and the Grants-in-Aid of the Ministry of Education, Science, Culture, and Sport, 13640238 (SM), 09874055 (MU).

REFERENCES

- Abramowicz, M. A., Czerny, B., Lasota, J. P., & Szuszkiewicz, E. 1988, *ApJ*, 332, 646
 Agol, E., Krolik, J., Turner, N. J., & Stone, J. M. 2001, *ApJ*, 558, 543
 Alme, M. L. & Wilson, J. R. 1976, *ApJ*, 210, 233
 Begelman, M. C. 1978, *MNRAS*, 184, 53
 Begelman, M. C. & Meier, D. L. 1982, *ApJ*, 253, 873
 Beloborodov, A. M. 1998, *MNRAS*, 297, 739
 Boller, T., Brandt, W. N., & Fink, H. 1996, *A&A*, 305, 53
 Borozdin, K., Revnivtsev, M., Trudolyubov, S., Shrader, C., & Titarchuk, L. 1999, *ApJ*, 517, 367
 Blondin, J. M. 1986, *ApJ*, 308, 755
 Colbert, E. J. M. & Mushotzky, R. F. 1999, *ApJ*, 519, 89
 Colpi, M. 1988, *ApJ*, 326, 223
 Eggum, G. E., Coroniti, F. V., & Katz, J. I. 1987, *ApJ*, 323, 634
 Eggum, G. E., Coroniti, F. V., & Katz, J. I. 1988, *ApJ*, 330, 142
 Flammang, R. A. 1984, *MNRAS*, 206, 589
 Frank, J., King, A., & Raine, D. 1985, *Accretion Power in Astrophysics* (Cambridge: Cambridge Univ. Press)
 Fujita, M. & Okuda, T. 1998, *PASJ*, 50, 639
 Fukue, J., Kato, S., & Matsumoto, R. 1985, *PASJ*, 37, 383
 Greiner, J., Cuby, J. G., & McCaughrean, M. J. 2001, *Nature*, 414, 522
 Hayashida, K. 2000, in *Proc. of 32nd COSPAR Meeting: Broad Band X-Ray Spectra of Cosmic Sources*, ed K. Makishima (*Adv. Space Research*), 25, 489
 Honma, F., Kato, S., & Matsumoto, R. 1991, *PASJ*, 43, 147
 Houck, J. C. & Chevalier, R. A. 1992, *ApJ*, 395, 592
 Kato, S., Fukue, J., & Mineshige, S. 1998, *Black-Hole Accretion Disks* (Kyoto: Kyoto Univ. Press)
 Katz, J. I. 1977, *ApJ*, 215, 265
 King, A. R., Frank, J., Kolb, U., & Ritter, H. 1997, *ApJ*, 482, 919
 Kley, W. & Lin, D. N. C. 1999, *ApJ*, 518, 833
 Koyama, A., Matsuda, T., Matsumoto, K., & Fukue, J. 1999, in *Star Formation 1999*, ed. T. Nakamoto (Nobeyama Radio Observatory) p.237
 Laor, A., Fiore, F., Elvis, M., Wilkes, B. J., & McDowell, J. C. 1997, *ApJ*, 477, 93
 Leighly, K. M. 1999, *ApJS*, 125, 317
 Lynden-Bell, D. & Pringle, J. E. 1974, *MNRAS*, 168, 603
 Makishima, K. et al. 2000, *ApJ*, 535, 632
 Matsumoto, H. et al. 2001, *ApJ*, 547, L25

- Mészáros, P. 2001, *Science*, 291, 79
- Mészáros, P., Rees, M. J., & Wijers, R. A. M. J. 1999, *NewA*, 4, 303
- Mihalas, D. & Klein, R. I. 1982, *J. Comput. Phys.*, 46, 97
- Mihalas, D. & Mihalas, B. W. 1984, *Foundations of Radiation Hydrodynamics* (Oxford: Oxford Univ. Press)
- Mineshige, S., Kawaguchi, T., Takeuchi, M., & Hayashida, K. 2000, *PASJ*, 52, 499
- Mineshige, S., Nomura, H., Hirose, M., Nomoto, K., & Suzuki, T. 1997, *ApJ*, 489, 227
- Mizuno, T., Ohnishi, T., Kubota, A., Makishima, K., & Tashiro, M. 1999, *PASJ*, 51, 663
- Narayan, R., Paczyński, B., & Piran, T. 1992, *ApJ*, 395, L83
- Narayan, R., Piran, T., & Kumar, P. 2001, *ApJ*, 557, 949
- Norman, C. & Scoville, N. 1988, *ApJ*, 332, 124
- Ohsuga, K., Umemura, M., Fukue, J., & Mineshige, S. 1999, *PASJ*, 51, 345
- Okada, K., Dotani, T., Makishima, K., Mitsuda, K., & Mihara, T. 1998, *PASJ*, 50, 25
- Okuda, T., Fujita, M., & Sakashita, S. 1997, *PASJ*, 49, 679
- Otani, C., Kii, T., & Miya, K. 1996 in *Röntgenstrahlung from the Universe* (MPE Report 263), ed H.U. Zimmermann, J.E. Trümper, H. Yorke (MPE Press, Garching) p.491
- Piran, T. 1999, *Physics Reports*, 314, 575
- Popham, R., Woosley, S.E., & Fryer, C. 1999, *ApJ*, 518, 356
- Pringle, J. E. 1981, *ARA&A*, 19, 137
- Ruffert, M., & Janka, H.-Th. 1999, *A&A*, 344, 573
- Rybicki, G. B. & Lightman, A. P. 1979, *Radiative Processes in Astrophysics* (New York: John Wiley & Sons, Inc.)
- Shakura, N. I. & Sunyaev, R. A. 1973, *A&A*, 24, 337
- Shakura, N. I., Sunyaev, R. A., & Zilitinkevich, S. S. 1978, *A&A*, 62, 179
- Spruit, H. C. & Ritter, H. 1983, *A&A*, 124, 267
- Stone, J. M., Mihalas, D., & Norman, M. L. 1992, *ApJS*, 80, 819
- Sunyaev, R. A. & Titarchuk, L. G. 1985, *A&A*, 143, 374
- Szuskiewicz, E., Malkan, M. A., & Abramowicz, M. A. 1996, *ApJ*, 458, 474
- Tanaka, Y. & Shibazaki, N. 1996, *ARA&A*, 34, 607
- Turner, N. J. & Stone, J. M. 2001, *ApJS*, 135, 95
- Umemura, M., Fukue, J., & Mineshige, S. 1998, *MNRAS*, 299, 1123
- Wang, J. M., Szuskiewicz, E., Lu, F. J., & Zhou, Y. Y. 1999, *ApJ*, 522, 839
- Wang, J.-M. & Zhou, Y.-Y. 1999, *ApJ*, 516, 420
- Watarai, K. & Fukue, J. 1999, *PASJ*, 51, 725
- Watarai, K., Fukue, J., Takeuchi, M., & Mineshige, S. 2000, *PASJ*, 52, 133
- Watarai, K., Mizuno, T., & Mineshige, S. 2001, *ApJ*, 549, L77
- Yamaoka, K., Ueda, Y., & Inoue, H. 2001, in *Proc. of X-Ray Astronomy in the New Century*, ed. H. Kunieda (PASP conf. series), in press